Nonlinear dynamics induced in a structure by seismic and environmental loading

Philippe Guéguen,[1,a)] Paul Johnson,[2] and Philippe Roux[1]
[1]*ISTerre, Université de Grenoble Alpes, CNRS/IFSTTAR, BP 53, 38041 Grenoble cedex 9, France*
[2]*Geophysics Group, Los Alamos National Laboratory, Los Alamos, New Mexico 87545, USA*

(Received 26 October 2015; revised 9 June 2016; accepted 30 June 2016; published online 26 July 2016)

In this study, it is shown that under very weak dynamic and quasi-static deformation that is orders of magnitude below the yield deformation of the equivalent stress−strain curve (around 10^{-3}), the elastic parameters of a civil engineering structure (resonance frequency and damping) exhibit nonlinear softening and recovery. These observations bridge the gap between laboratory and seismic scales where elastic nonlinear behavior has been previously observed. Under weak seismic or atmospheric loading, modal frequencies are modified by around 1% and damping by more than 100% for strain levels between 10^{-7} and 10^{-4}. These observations support the concept of universal behavior of nonlinear elastic behavior in diverse systems, including granular materials and damaged solids that scale from millimeter dimensions to the scale of structures to fault dimensions in the Earth. © *2016 Acoustical Society of America*. [http://dx.doi.org/10.1121/1.4958990]

[JFL] Pages: 582–590

I. INTRODUCTION

Seismic wave perturbations, if strain amplitude is sufficiently large, can induce deformation in solids. In solids, granular materials and structures, the effect is a transient-induced disequilibrium, where the material modulus decreases and the dissipation increases, and which may become permanent if deformations are large or frequent. Materials also commonly exhibit a fascinating, slow dynamical recovery from disequilibrium to the original or a new equilibrium of the system's elastic properties after strong wave deformations terminate, observed in the laboratory on rocks (e.g., Guyer and Johnson, 1999; Johnson and Sutin, 2005; TenCate, 2011; Renaud *et al.*, 2012; Renaud *et al.*, 2014), in concrete materials (e.g., Lacouture *et al.*, 2003; Bentahar *et al.*, 2006; Bui *et al.*, 2013), at the Earth's surface in soils (e.g., Field *et al.*, 1997; Sawazaki *et al.*, 2009; Wu *et al.*, 2009a; Ohmachi and Tahara, 2011; Johnson *et al.*, 2009; Renaud *et al.*, 2014) and at the scale of the Earth's crust (Peng and Ben-Zion, 2006; Karabulut and Bouchon, 2007; Brenguier *et al.*, 2008; Wu *et al.*, 2009b). Between laboratory and crustal scales, we studied an intermediate scale system: a civil engineering structure. To first order, a building's natural frequency and damping depend on the Young's modulus of the equivalent one dimensional (1D) system and, assuming constant mass, its dynamic response obeys Newton's second law (Chopra, 2007). Monitoring these values therefore enables the assessment of rapid damage of the elastic nonlinear response of the structure, after an extreme event (Clinton *et al.*, 2006; Michel and Guéguen, 2010), or in a situation of slow deterioration due to ageing (Kashima and Kitagawa, 2006). In this study, the variations of elastic properties of the Factor building (UCLA campus, California) are analyzed under weak deformation induced by dynamic (e.g., earthquake) and quasi-static (e.g., atmospheric) loadings. After a brief description of the building and data, frequency and damping are extracted over four months of continuous ambient vibrations recorded at the top of the building. Assuming as a first order approximation a 1D single-degree-of-freedom (SDOF) structure, the method used for the frequency and damping assessment is presented and the elastic parameter variation is described in connection with the amplitude of loading. Finally, the apparent universal nonlinear elastic behavior of diverse systems is discussed.

II. DATA FROM THE UCLA FACTOR BUILDING

We analyzed vibrations recorded at the top of the UCLA Factor building (California) between September and December 2004. The building is a steel structure, designed and built in the 1970s, comprising a moment-resisting frame structure with a total height of 66 m and a rectangular shape (surface area 5×10^3 m^2). After the Mw7.1 Northridge earthquake (1994), a network of 72 sensors was installed by the U.S. Geological Survey (USGS), and renovated in 2003 with a more sensitive acquisition system, comprising force-balance accelerometers (Episensors) and 24-bit multi-component stations in order to enable the analysis of ambient vibrations (Kohler *et al.*, 2005). This new configuration provides continuous data. The recordings were sampled at 100 Hz and acquisition was synchronized by GPS. In this study, we used data from two stations that are located on the top (floor 15) to estimate the frequency and damping corresponding to the fundamental bending mode in the horizontal (longitudinal) direction, and on the ground to estimate the strain in the same direction. Sensors are located at the east corner of the building, oriented northwards in its longitudinal direction. In this building, Kohler *et al.* (2005) inferred torsion and higher modes but we focus our analysis on the frequency and

[a)]Electronic mail: philippe.gueguen@ujf-grenoble.fr

 0001-4966/2016/140(1)/582/9/$30.00

damping of the fundamental mode because of the high sensitivity of this mode to change related to the effective mass (Farrar *et al.*, 2001) and of the energy contained within the fundamental modes (i.e., its modal participation factor) which aids in a good signal to noise ratio. This is confirmed with numerical simulation and laboratory experiments using the same signal processing technique (Roux *et al.*, 2014). Moreover, previous modal analysis of ambient vibrations or earthquake data recorded in the building showed an apparent modal frequency of 0.59 Hz and damping ratio of 2% (Kohler *et al.*, 2005; Nayeri *et al.*, 2008; Skolnik *et al.*, 2006) corresponding to the fundamental horizontal mode of vibration of the soil–structure system in the longitudinal direction that will be analyzed in this study.

III. DATA PROCESSING

In order to monitor the variations of apparent frequency and damping of the fundamental mode, the impulse response of the structure was obtained by segmenting the data into time windows of identical length. The random decrement technique (RDT) was used, a commonly applied method based on the stationary and random nature of vibrations to extract the structure's impulse response (Cole, 1973). This method considers that the observed signal $s(t)$ contains random and stationary noise, mixed with the impulse response of the structure subjected to a very low level of excitation. Considering a building as a linear one-dimension single degree of freedom system (1D-SDOF), the equation of its response v(t) is governed by the following equation:

$$\ddot{v}(t) + 2\zeta\omega\dot{v}(t) + \omega v(t) = -v''_g, \tag{1}$$

with ω the specific angular frequency, ζ the damping ratio of the system, v''_g the input motion. Considering a triggering condition termed $T_{x(t)}$, the stationary modal response of the 1D-SDOF can be expressed as the sum

$$v(t) = v_1(t) + v_2(t), \tag{2}$$

where v_1 and v_2 correspond to the forced (stochastic part) and free (deterministic part) responses of the system after $T_{x(t)}$, respectively. Derived from the Duhamel's integral solution which expresses the response of a damped system to a general loading, the solution of v_1 is the convolution of the unit-impulse response function of the SDOF $g(t)$ and the loading after $T_{x(t)}$ at time t_0, i.e.,

$$v_1(t) = \int_{t_0}^{t} g(t - t_0 - \tau)v''_g d\tau, \tag{3}$$

v_2 corresponds to the free oscillation response of the SDOF and is expressed by the equation

$$v_2(t) = \left[v(0)\cos\omega_D t + \frac{\dot{v}(0) + v(0)\zeta\omega}{\omega_D}\sin\omega_D t\right]e^{-\zeta\omega t}, \tag{4}$$

with ω_D the free-vibration frequency of the damped system, nearly equal to ω for low damping value (<20%), and $v(0)$,$v(0)$ the initial conditions $T_{x(t)}$ at time t_0. The mathematical expectation of the response of the SDOF after t_0, for a given initial triggering condition $T_{x(t0)}$, noted $E[v(t-t0)|T_0]$, is given by

$$E[v(t - t_0)|T_0] = E[v_1(t - t_0)|T_0] + E[v_2(t - t_0)|T_0]. \tag{5}$$

Assuming an ergodic process, each segment after t_0 can be considered as a sample function of the stationary modal response of the SDOF. According to the stationary and stochastic nature of the loading $v''_g(t)$ (i.e., ambient vibrations), the mathematical expectation of the stochastic part v_1 is constant. In contrast, the deterministic part of the response v_2 is only dependent on the modal parameters of the SDOF, i.e., the frequency and the damping, assumed constant per segment, i.e., during the time length of the signal. Thus, $E[v(t - t_0)|T_0]$ corresponds to the free-response of the SDOF, called the random decrement (RD) signature. Averaging the time window of the signal $s(t)$ recorded at the top of the building leads to the deterministic part of the response, i.e.,

$$\mathrm{RDT}(t) = \frac{1}{N}\sum_{i=1}^{N} s(t_i + \tau)|\, T_0, \tag{6}$$

with τ the duration of each window, N the number of segments. By stacking a large number N of windows of duration τ whose initial conditions T_0 are identical to ensure the positive contribution of each window [for example, $s(t_0) = 0$], the coherent average magnifies the impulse response when compared to uncorrelated noise (Fig. 1). The RD converges toward the impulse response of the structure $g(t)$, which can be modeled as

$$g(t) = \frac{1}{m\omega_D}e^{-\zeta\omega t}\sin(\omega_D t)\ t > 0, \tag{7}$$

where m is the mass of the structure. In the rest of the document we will consider that the structure's impulse response is stationary over N and the frequency and damping values reflect the state of the structure. Figure 1 displays two examples of the RDT process, for time slots corresponding to two loading cases showing the ability to detect small variations of frequency by RDT. As shown in Eq. (7), the structure's response $g(t)$ decreases exponentially by the function $e^{-\zeta\omega t}$ according to the system frequency and damping (Chopra, 2007) and represents the response of the overall mechanical system. The Fourier transform $G(\omega)$ corresponds to the transfer function of the system and the shift of the resonance peak as well as the widening of the peak shape reflect the evolution of its elastic properties. Once the RDT has been calculated, frequency ω is obtained by a zero-crossing method applied to $g(t)$ and damping ζ from the average decrease in amplitudes using the traditional logarithmic decrement method (Chopra, 2007). The choice of initial conditions, number of stacked windows N and the filter to be applied must be determined before RDT processing. In the present case, we followed the hypotheses proposed by Asmussen *et al.* (1999) and confirmed by Mikael *et al.* (2013) and

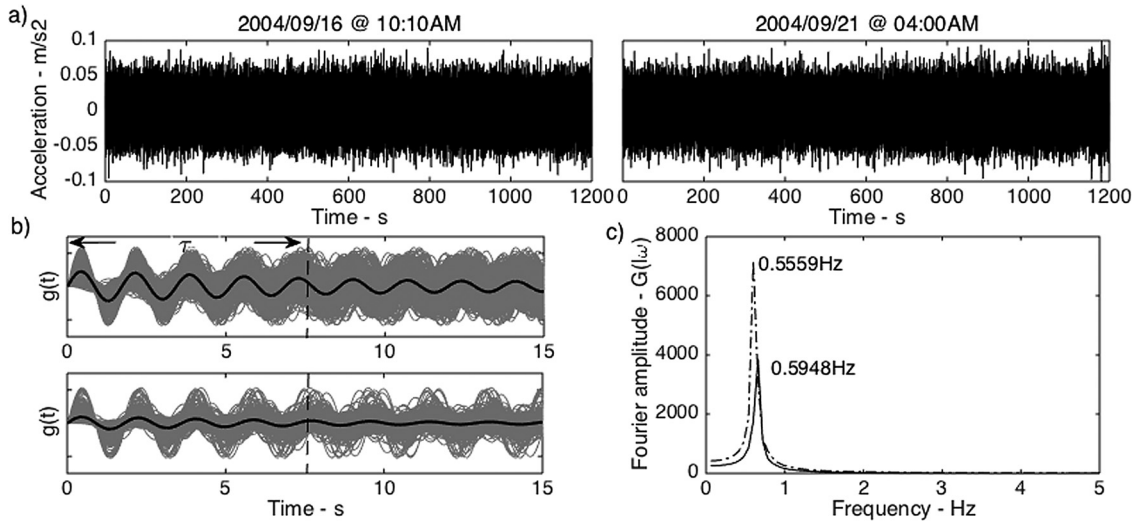

FIG. 1. Description of the random decrement technique (RDT) used in this study for two different time periods showing frequency variation. (a) Example of 20-min long windows of ambient vibrations recorded at the top of the Factor building in the longitudinal direction. (b) Random decrement signature of the first (2004/09/14, upper row) and second (2004/09/21, lower row) window. Gray lines are the N stacked windows of length τ [Eq. (5)]. Black line is the result of the stack that corresponds to the impulse response $g(t)$ of the system, used for frequency and damping assessment [Eq. (6)]. Before the stacking process, a band-pass filter is applied between 0.4–0.7 Hz (see text for details). (c) Transfer function $G(\omega)$ of the two time periods with the value of the two frequency peaks and assessment of the frequency peak (solid line: window September 16, 2004 at 10:10 a.m.; dashed line: window September 21, 2004 at 04:00 a.m.). Black arrows in Fig. 2 indicate the two periods.

Nasser *et al.* (2016) for processing the Factor building data. The hypotheses are assumed as being suitable to continuous ambient vibrations data recorded at the top of a building. These hypothesis are (1) as initial conditions, we considered zero acceleration and positive velocity, i.e., each zero-crossing time toward the positive acceleration; (2) a length of window τ corresponding to at least four periods of the system; and (3) a minimum number of windows N corresponding to the entire duration of the windows equal to at least 1000 periods. In the specific case of the UCLA Factor

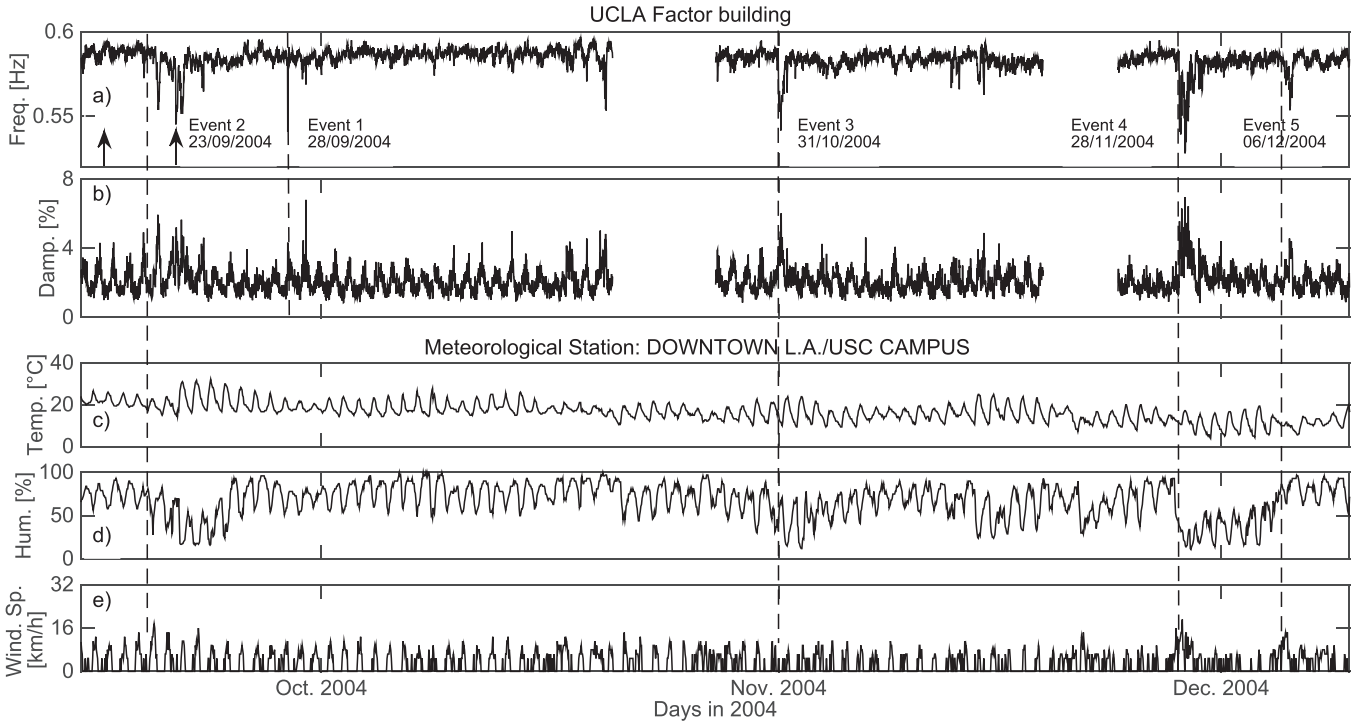

FIG. 2. Variation of the fundamental frequency (a) and associated damping (b) of the UCLA Factor building from September to December 2004, in the longitudinal direction (north–south). Frequency and damping were calculated using the random decrement technique, on 20-min windows, after filtering between 0.4 and 0.7 Hz. The interruptions correspond to time periods for which no data were available. Five significant loadings are indicated (events 1 to 5). Event 1 corresponds to the Parkfield earthquake. Frequency and damping are compared with meteorological data (c) air temperature, (d) humidity, and (e) wind speed recorded around 15 km from the Factor building (USC Campus station, U.S. National Climate Data Center, http://cdo.ncdc.noaa.gov/ulcd/ULCD). Dashed lines indicate four meteorological events (Nos. 2–5) and one earthquake (No. 1). Black arrows indicate the time of the windows used as example in Fig. 1.

TABLE I. Main features of the events discussed in the manuscript. (Wind: wind speed; Temp: Air temperature; Hum: Air humidity; Acc Top: maximal acceleration recorded at the top of the structure; Strain: maximal strain computed as the relative displacement between top and bottom; t_{max}: duration of the recovery observed in Fig. 4).

No.	Date	Wind (km/h)	Temp. (°C)	Hum. (%)	Acc Top (cm/s^2)	Strain 10^{-5}	t_{max} (h)
	$\mu\|\sigma$	4.4|1.5	16.5|4.2	66.5|19.3			
1	Sept. 28, 2004	4.1	18.9	72.6	2.1	3.0	3
2	Sept. 19, 2004	5.5	21.9	44.4	0.4	0.4	12
3	Oct. 31, 2004	3.7	16.7	44.2	0.3	0.5	20
4	Nov. 27, 2004	4.8	10.9	34.5	0.6	0.9	21
5	Dec. 4, 2004	4.2	10.7	82.1	0.2	0.2	13

building, the period of the fundamental mode is approximately 1.7 s (Kohler *et al.*, 2005; Skolnik *et al.*, 2006), and we consider the RDT calculation over constant 20-min windows. In the presence of transient vibrations (i.e., earthquakes), the windows used for the RDT may be longer than the duration of the earthquake shaking. The change in the frequency and damping on the window during which seismic waves from the earthquake take place is equivalent to the average of this variation, the instantaneous changes being more pronounced.

Before the stacking process, a filter was applied, centered on the frequency of the system to be identified to eliminate possible frequency beating in the impulse response caused by mixing close modes. The filter width must enable good assessment of damping. The latter is proportional to the width of the peak of the impulse function at −3 dB of maximal amplitude. Supposing damping of around 5% in first approximation, the filter width must be at least +/−10%. Based on previous published studies, we selected 0.4–0.7 Hz similar to the cutoff frequencies of 0.45 Hz and 0.65 Hz used by Kohler *et al.* (2005) for the fundamental mode of the UCLA Factor building. Only the signal recorded at the top is used to extract frequency and damping. In parallel to the frequency and damping analysis, total strain was computed as the maximal relative displacement obtained by the difference of the top (sensor floor 15) and bottom (sensor on the ground) displacement normalized by the building height. The acceleration to displacement calculation was done following Boore (2005), i.e., removing the trend and mean, tapering with a 5% Tukey window and applying zero padding.

IV. FREQUENCY AND DAMPING VARIATION

Figures 2(a) and 2(b) show the evolution of frequency and damping of the fundamental horizontal mode in the longitudinal direction over four months of recording. The mean features of the events discussed herein are given Table I. We observed average stability of measurements, indicating a fluctuation around the average system values, i.e., 0.583 Hz (+/−0.008 Hz) and 2.22% (+/−0.86%) corresponding to a variation coefficient (σ/μ) 1% and 38%. Compared to the frequency analysis previously mentioned, we found that RDT provides an efficient solution for tracking very small variations in the elastic properties of vibrating civil engineering systems, associated with day/night temperature variations in particular, as observed previously by other authors (Kohler *et al.*, 2005; Nayeri *et al.*, 2008). The recovery of frequency and damping is also observed in direct relationship with the traditional relation of a simple oscillator with one degree of freedom [$\omega^2 = k/m$; $\zeta = C/(2\omega m)$, where C controls the damping]. In fact, for constant mass, frequency and damping are proportional and inversely proportional to the rigidity of the structure, respectively, and therefore depend amongst other things on its elastic properties, on its design and its coupling with the ground.

This is made evident by the dynamic forcing of the Parkfield earthquake [Event 1, Figs. 2 and 3(a)], which caused an immediate (i.e., instantaneous activation) and rapid (i.e., quickly reaching the minimum value) softening of the frequency and an increase of damping under weak (elastic) deformation. In fact, the Parkfield earthquake induced relatively low levels of acceleration (ground acceleration: 10^{-2} m/s^2 – top: 2×10^{-2} m/s^2) and displacement (ground

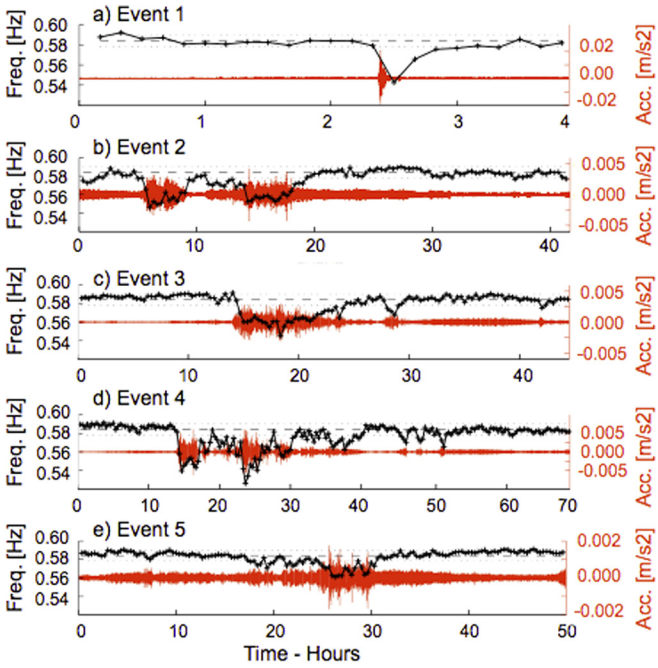

FIG. 3. (Color online) Zoom of the variation of the fundamental frequency of the UCLA Factor building over time for the five events identified in Figs. 2. (a)–(e) correspond to event 1 to event 5, respectively. The solid black line represents the average frequency value, calculated over each 20-min window, whose centers are indicated by a cross. The dotted and dashed lines correspond to the average and standard deviation of frequencies, respectively. The red lines show the acceleration measured at the top of the building (station FA.FABI.FE.HNN). Note that the events have different durations.

displacement: 7×10^{-4} m – top: 2×10^{-3} m), corresponding to a strain below 10^{-4} and no structural damage was reported. After RDT processing, additional strong and slow variations of frequency and damping were observed as shown in Fig. 2 that were not associated with seismic events. In contrast to dynamic loading, equivalent frequency variations in response to quasi-static forcing are observed [Events 2 to 5, Figs. 2 and 3(b)–3(e)], i.e., characterized by a slow rate of variation of frequency and damping compared to those induced by the Parkfield dynamic loading and staggered over several days. In our case, the distinction between dynamic and quasi-static is related to the variation rate of the loading, proportional to the ratio amplitude versus duration and equivalent to what is observed in dynamic acousto-elastic testing (e.g., Renaud *et al.,* 2014). In contrast to dynamic loading, quasi-static loading in engineering buildings means that the load is applied so slowly that the structure deforms with a very low strain rate without producing inertia forces. These variations occur at time corresponding to a quasi-static equivalent variation in air humidity and wind speed parameters recorded at the Los Angeles CQT weather station [Figs. 2(c)–2(e) located at University of Southern California Campus downtown, about 15 km east to the Factor building. It is known that variations in meteorological conditions can modify the soil foundation in some types of actual building and therefore the structure's anchoring conditions (Clinton *et al.,* 2006; Todorovska and Al Rjoub, 2006). Indeed, under elastic conditions, the apparent overall response observed at the top of the system (f_{app}, ζ_{app}) can be related (Luco *et al.,* 1987) to the fundamental fixed-based frequency (f_1, ζ_1) by the combination of a horizontal translation mode (f_H, ζ_H) and a rocking mode (f_R, ζ_R) of a rigid building on flexible soil, and consequently influenced by the coupling between the soil and the structure. Snieder and Safak (2006) supported that the value of the structure frequency, i.e., f_1, can be isolated by deconvolution between the top and the bottom recordings, thus eliminating partially the influence of the soil−structure interaction considering a model without rocking motion. In our case, we partially removed the influence of the seismic input by computing deconvolution carried out using the water level regularization technique (Clayton and Wiggins, 1976). Assuming the input and the output of the signal are known as the recorded time histories at the bottom and top of the structure, the deconvolved impulse response of the fixed-base structure is computed as follows:

$$h(t) = \mathrm{FT}^{-1}\left\{\frac{O(\omega)}{\max\left\{I(\omega), k\left(|I(\omega)|, \frac{I(\omega)}{|I(\omega)|}\right)_{\max}\right\}}\right\}, \quad (8)$$

where FT^{-1} denotes inverse Fourier transform, O and I the output and input signal, respectively, and k the water level coefficient ($k = 0.10$ in our case). The RDT method was applied to the deconvolved vibration at the building top and comparable values of f_1 and f_{app} were obtained, allowing us to infer negligible soil — structure interaction ($f_1 = 0.583$ Hz +/− 0.010 Hz – $\zeta_1 = 2.69\%$ +/− 1.58%). For that reason, in the following, the modal parameters of the structure alone are not considered and the apparent parameters (f_{app} and ζ_{app}) are termed frequency and damping ratio. Finally, the trend of the apparent frequency and damping variations under atmospheric events is unusual especially for such small loading. Our results suggest that meteorological effects induced weak and slow vibrations that weaken the elastic properties of the building, comparable to what happens for an equivalent dynamic but quasi-static forcing (i.e., a slow forcing). Because of the distance between the building and the weather station, it is not possible to make a quantitative correlation of the weather conditions with the frequency variation or deformation of the structures. The weather station does not capture local and transient fluctuations right to the building and only a general trend can be described.

V. SLOW DYNAMICS ASSOCIATED WITH DYNAMIC AND QUASI-STATIC LOADING

In Fig. 3, we show an expanded view over time of the five events selected in Fig. 2. For all events, the window of the time history of the building top acceleration is displayed synchronized with the frequency variation. Because of the quasi fixed-based structure condition, acceleration, strain and displacement have equivalent trends and only acceleration is shown in Fig. 3. In all cases, a rapid decrease in resonance frequency corresponding to the beginning of the system loading is observed, followed by a slow recovery to the initial elastic properties, strongly similar to the slow dynamics observed under laboratory conditions in rock and unconsolidated granular material (e.g., Johnson and Sutin, 2005; Guyer and Johnson, 2009; TenCate, 2011; Bui *et al.,* 2013; Renaud *et al.,* 2012). In the case of repetitive reloadings, as for events 2, 3, and 4, we observe similar behaviors, i.e., a rapid decrease at the beginning of the loading followed by a slow recovery. Furthermore, we observe that, for continued loading as in the case of the meteorological events, the frequency and therefore the elastic (Young) modulus remain at a sustained low value until the forcing ceases. This is strongly suggestive of the "conditioning phenomenon" observed in the laboratory, where the oscillatory forcing reduces the elastic modulus until it is terminated (e.g., Guyer and Johnson, 2009; TenCate, 2011).

It is interesting to note that the quasi-static forcing due to changes in meteorological conditions produces a softening effect. Meteorological parameters are usually strongly linked and it is not the goal of this paper to separate each effect. However, as shown in red in Fig. 3, meteorological forcing induces vibrations with higher amplitude than for building vibration with only background noise forcing. Several papers (e.g., Banerjee, 1924) reported observations of the increase of seismic noise correlated with oceanic and atmospheric events. Roux (2009), Hillers *et al.* (2012), and Beucler *et al.* (2015) showed the event impact in different frequency bands, while Stelhy *et al.* (2006) reported 5–10-s pressure variation period in the micro-seismic noise originating from the Pacific ocean, a frequency band of excitation that is close to the resonance frequency of the Factor building. With the instrumentation available at the bottom of the building (i.e.,

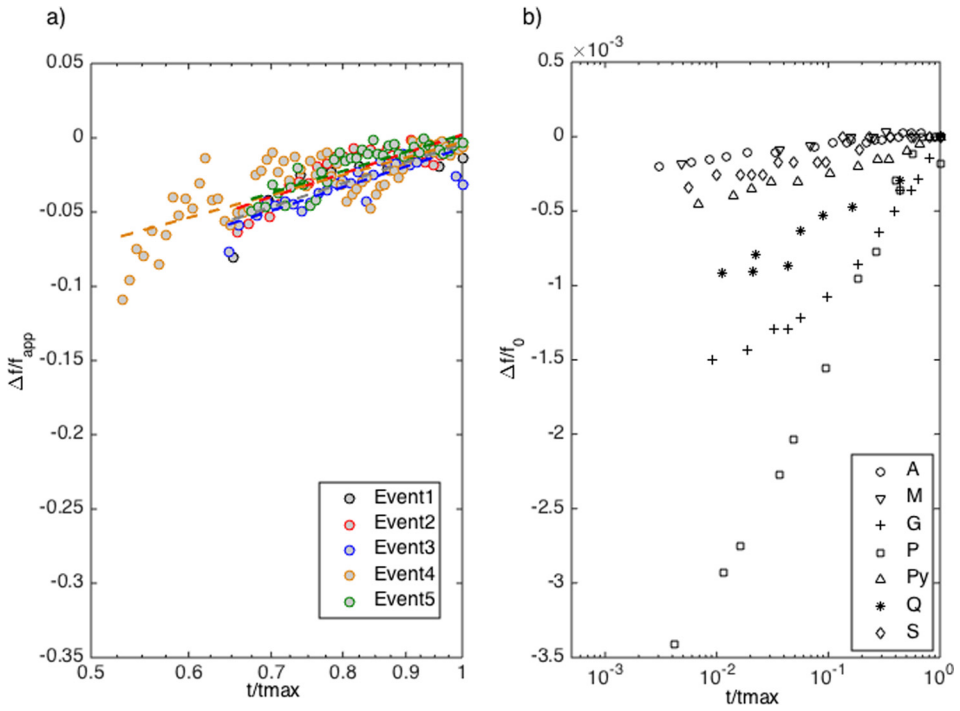

FIG. 4. (Color online) Log-linear rate of recovery for (a) the Factor building for the five events and (b) diverse solids tested in the laboratory by Johnson and Sutin (2005). The *Y*-axis is the variation of the normalized frequency $(f-f_{app})/f_{app}$ and the *X*-axis is the normalized variation of t/t_{max}. t_{max} is the time need for recovery computed between original time and time of the end of recovery. For each event, the original time of recovery is arbitrarily chosen as the time corresponding to the minimum value of the frequency and the end of recovery is when frequency recovers the value of the building's apparent frequency f_{app}. The dashed lines (a), showing the same slope, give the log-linear rate of recovery. Data dispersion are related to the re-loading of the structure during recovery. In (b) solid samples under study are A: alumina ceramic; M: marble; P: Perovskite ceramic; G: Pearlite/graphite metal; S: sintered metal; Q: quartzite; Py: Pyrex containing cracks.

4 g full scale accelerometer), ocean induced seismic noise is not visible and this assumption cannot be tested by the actual data. Clinton *et al.* (2006) and Herak and Herak (2010) reported a softening effect in relation with the wind speed. In our case, the amplitude of acceleration is very weak and under normal circumstances, nonlinearity in the material would be expected to harden the system at such a low level of strain, corresponding to an increase in modal frequency. We posit that there is a softening effect due to the induced vibration that forces softening nonlinearity. A conceptually similar effect has been observed in glass bead packs under circular shear, where internal vibrations generated by grain collisions produce bulk softening (van der Elst *et al.*, 2012).

As in laboratory experiments or at the scale of the Earth's crust, the explanation for the slow dynamics observed here might be linked to the internal strain energy created during the fast dynamics, and might certainly be related to the processes that cause creep in granular materials (Rutter, 1983; Johnson and Jia, 2005) or damage in fault zones after earthquakes (Peng and Ben-Zion, 2006; Wu *et al.*, 2009b; Brenguier *et al.*, 2008; Karabulut and Bouchon, 2007). In all cases, the existence of "cracks" at different scales—micro-cracks, macro-cracks, and/or contact mechanics—has been shown to be fundamental (Baish and Boeckelmann, 2001; Pasqualini *et al.*, 2007) to the slow recovery effect. In structures, we believe that the primary mechanism may be due to heterogeneous regions associated with steel connections as well as the contribution of cracked concrete, which could be a key-issue to the future monitoring of structure health.

A remarkable point is the apparent scale invariance of the nonlinear behavior, which is highly similar in samples that are millimeters in diameter (laboratory scale) (e.g., Guyer and Johnson, 2009) up to the scale of the crust in the vicinity of fault zones (e.g., Brenguier *et al.*, 2008), showing a modulus decrease due to fast dynamical excitation and slow recovery. The fast and slow dynamics effects are distinguished according the rate of variation. We observe very different time scales than those observed in the Earth, i.e., minutes−hours versus months−years for the seismic loading and the atmospheric loading, respectively, but the sense of recovery appears to be the same, i.e., approximately linear with the log of time (Fig. 4). The time scales are very similar to those observed in laboratory studies of rock and granular material, however. The log-linear rate of recovery is also the same for the UCLA Factor building [Fig. 4(a)], providing an intermediate scale result to the apparent universality of nonlinear behavior. In the present case [Fig. 4(a)], the recovery slope remains the same whatever the forcing event, while for diverse solids tested in the laboratory by Johnson and Sutin (2005) [Fig. 4(b)], the rate of recovery is different, because the recovery depends upon the material elasticity. This notion is quantitatively supported by numerous laboratory experiments (e.g., Guyer and Johnson, 2009; Renaud *et al.*, 2012). This property should be confirmed in further analysis carried out in different types of building but the results may have wide applicability for investigating the internal properties of damaged building.

VI. NONLINEAR ELASTICITY

At this stage, the mechanisms for nonlinear elastic behavior in structures are not fully understood, but their monitoring provides insight to the dynamics of structures. The relationship between deformation and damage is generally the foundation of all methods to estimate structural integrity after an earthquake. Concrete deforms rapidly by cracking under shear, and steel absorbs the forces until plastification occurs under high loads. Thus, the structural response exhibits approximately bi-linear elasto-plastic behavior. In the case of forcing caused by the Parkfield earthquake (Fig. 5),

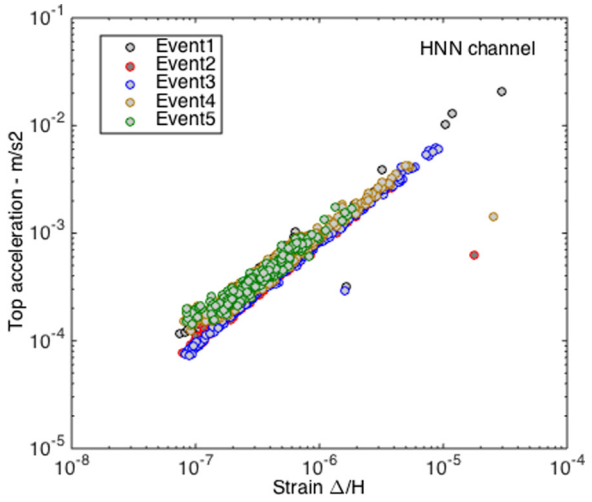

FIG. 5. (Color online) Acceleration at the top of the building versus the deformation (Δ/H) calculated as the displacement difference between the top and bottom of the structure, divided by its height. This curve is proportional to the stress–strain response. The five events from Fig. 1 are shown for north–south acceleration component (HNN channel).

the average internal strain experienced by the structure is around 10^{-4}, a value well below the deformation generally assumed to induce a nonlinear response (ductile), according to engineering prediction techniques such as the HAZUS Technical Manual (1999) on which most methods for assessing the vulnerability of existing structures are based.

For the Factor building, the yield point of the bi-linear equivalent behavior model given by HAZUS for this type of building is assumed to correspond to a global strain around 3×10^{-3}. This value ultimately corresponds to the deformation beyond which the structure is permanently damaged. Remarkably, significant elastic nonlinear behavior is observed for the very lowest levels of deformation (Fig. 6). In this case, the deformation is computed as the maximum relative displacement between the top and bottom of the building observed for each 20-min time slot and normalized by the building height. The observed dependency of the frequency variation as a function of deformation between 10^{-7} for the quasi-static events (Event 2 to 5) and 10^{-4} for the dynamic event (Event 1), is typical of the signature of nonlinear mesoscopic elasticity (NME) observed in samples of rock and unconsolidated granular material analyzed in laboratory conditions (e.g., Guyer and Johnson, 1999; Ostrovsky and Johnson, 2001; Guyer and Johnson, 2009 and references therein) as well as other, diverse solids (e.g., Johnson and Sutin, 2005). NME materials exhibit elastic properties determined by a bond system heterogeneous in size and shape with contacts between rigid grains or asperities along cracks resulting in the nonlinear elastic behavior. Despite the fact that the scale is different, the building response is directly analogous to laboratory samples, experiencing loading and unloading under the influence of seismic (dynamic) or atmospheric (quasi-static) forcing, which induces a typical response in all NME materials (Fig. 6).

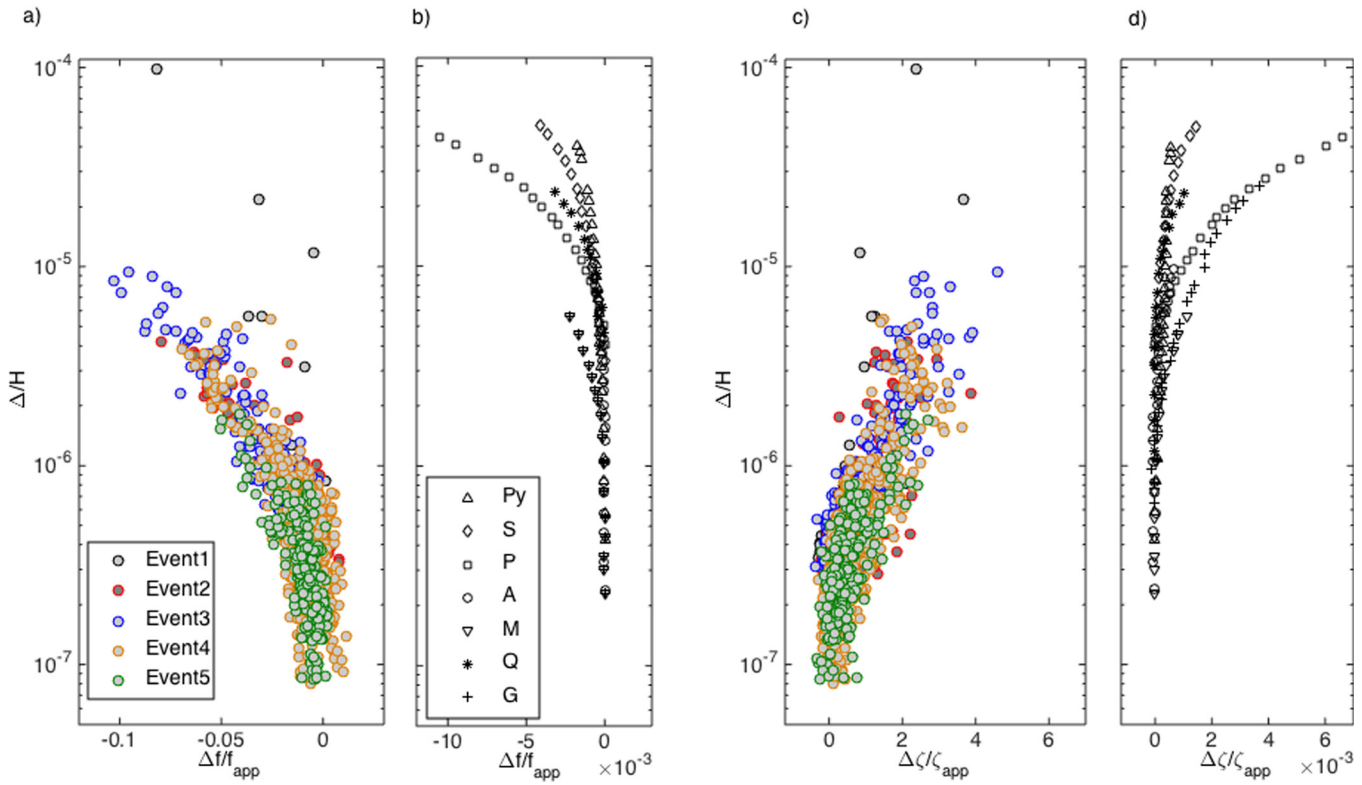

FIG. 6. (Color online) Variation of the normalized frequency $(f - f_{app})/f_{app}$ (a) and the associated damping $(\zeta - \zeta_{app})/\zeta_{app}$ (c) corresponding to the time windows of Fig. 2 as a function of deformation (Δ/H) calculated as the displacement difference between the top and bottom of the structure, divided by its height. The five events indicated previously are taken into account, considering the north–south direction of acceleration only (HNN code channel). In this figure, the apparent response is considered by applying the RDT method to the top recording. Equivalent nonlinear fast dynamics laboratory-scale results for diverse solids are given for comparison according to Johnson and Sutin (2005) in frequency (b) and damping (d) (A: alumina ceramic; M: marble; P: Perovskite ceramic; G: Pearlite/graphite metal; S: sintered metal; Q: quartzite; Py: Pyrex containing cracks).

An equivalent relationship is observed for damping, inversely proportional to that of frequency. Damping is exceptionally complex (Crandall, 1970), since it represents the combination of viscous damping of materials, radiation damping at the point of contact between the ground and the structure and probably diffusion damping around the points of structural heterogeneity (connecting points between walls and floors, for example) or material heterogeneity (cracks and impedance contrasts between materials). We also note [Figs. 6(a) and 6(c)] that, for the Parkfield earthquake, reduction in frequency (and increase in damping) was less significant for a given strain than that produced by meteorological events. Frequency and damping variations depend on the energy of the relative response concentrated around the apparent resonant frequency of the soil−structure system and proportional to the strain amplitude. The loading (or the strain) is significantly larger during the Parkfield event than during the meteorological events, but the frequency changes are similar. In the same manner, under relatively smaller dynamic loading magnitudes (atmospheric loading), the amplitude of damping is equivalent for Parkfield but the variation for equivalent strain is less remarkable for this "fast" event [Fig. 6(c)]. However, compared to nonlinear laboratory material [Fig. 6(d)], the same trend of variation is observed, but with a smaller variation for equivalent strain value (factor 1000 for damping and 10 for frequency). As noted in Fig. 4(a), the rate of recovery is the same in the structure and, as reported at different scale by previous studies, might be representative of the micro- or macro-scale state of the system, such as the opened/closed cracks, structural joints, etc., that might be responsible for the nonlinear and slow dynamic response of the Factor building.

VII. CONCLUSION

With the exception of materials such as Plexiglas, glass beads, or rocks, few systems, particularly coupled systems such as engineering structures, have had their slow dynamic elastic behavior examined in detail. The dynamical-forcing from the Parkfield earthquake shown here are very similar to laboratory results. The meteorological forcing is fascinating because it induces dynamical motion and in turn softening and recovery. The observations were made possible through the use of a robust signal processing method (the RDT). The localization along the building of the softening could be tested using mode-shape based methods, but is beyond the scope of this study. Moreover, it is not clear what the weather parameter is that essentially controls the variation of the frequency and damping, and further works must be carried out for that. Thanks to the availability of new continuous data acquired by increasingly sensitive instruments, the simultaneous and accurate measurement of frequency and damping of a structure provides new information with potential for improving the characterization of the seismic response of existing structures and the assessment of their post-earthquake integrity. Changes in design and construction practice to ensure safer, more resistant buildings are often a direct result of such observations (Corneiro, 2006). Furthermore, these observations also eliminate the doubt remaining over certain variations observed that should not be interpreted as damage indicators or degradation due to ageing, but as natural fluctuations associated with nonlinear elastic response. Moreover the results bridge the scales between the laboratory and Earth where dynamic elastic nonlinearity has been observed, lending support to the concept of nonlinear mesoscopic elasticity universality class.

ACKNOWLEDGMENTS

All of the data used in this study came from the UCLA Factor building array downloaded from the IRIS (http://www.iris.edu) datacenter, mseed code FABI.FE.HNN and FABA.XE.HNN. P.G. acknowledges LabEx OSUG@2020 (Investissements d'avenir - ANR10LABX56). P.J. acknowledges support by the U.S. Department of Energy, Office of Science, Office of Basic Energy Sciences, Chemical Sciences, Geosciences, and Biosciences Division. P.R. acknowledges the European Research Council through the advanced grant "Whisper" 227507.

Asmussen, J. C., Brincker, R., and Ibrahim, S. R. (**1999**). "Theory of the vector random decrement technique," J. Sound Vib. **226**(2), 329–344.

Baisch, S., and Bokelmann, G. H. (**2001**). "Seismic waveform attributes before and after the Loma Prieta earthquake: Scattering change near the earthquake and temporal recovery," J. Geophys. Res.: Solid Earth **106**(B8), 16323–16337, doi:10.1029/2001JB000151.

Banerjee, S. K. (**1924**). "Microseisms associated with the incidence of the South-West monsoon," Nature **114**, 576.

Bentahar, M., El Aqra, H., El Guerjouma, R., Griffa, M., and Scalerandi, M. (**2006**). "Hysteretic elasticity in damaged concrete: Quantitative analysis of slow and fast dynamics," Phys. Rev. B **73**(1), 014116.

Beucler, E., Mocquet, A., Schimmel, M., Chevrot, S., Quillard, O., Vergne, J., and Sylvander, M. (**2015**). "Observation of deep water microseisms in the North Atlantic ocean using tide modulations," Geophys. Res. Lett. **42**(2), 316–322, doi:10.1002/2014GL062347.

Boore, D. (**2005**). "On pads and filters: Processing strong-motion data," Bull. Seismol. Soc. Am. **95**(82), 745–750.

Brenguier, F., Campillo, M., Hadziioannou, C., Shapiro, N. M., Nadeau, R. M., and Larose, E. (**2008**). "Postseismic relaxation along the San Andreas Fault at Parkfield from continuous seismological observations," Science **321**, 1478.

Bui, D., Kodjo, S. A., Rivard, P., and Fournier, B. (**2013**). "Evaluation of concrete distributed cracks by ultrasonic travel time shift under an external mechanical perturbation: Study of indirect and semi-direct transmission configurations," J. Nondestruct. Eval. **32**(1), 25–36.

Chopra, A. (**2007**). *Dynamics of Structures* (Prentice Hall, Englewood Cliffs, NJ).

Clayton, R. W., and Wiggins, R. A. (**1976**). "Source shape estimation and deconvolution of teleseismic bodywaves," Geophys. J. R. Astron. Soc. **47**, 151–177.

Clinton, J. F., Bradford, S. C., Heaton, T. H., and Favela, J. (**2006**). "The observed wander of the natural frequencies in a structure," Bull. Seism. Soc. Am. **96**, 237–257.

Cole, H. (**1973**). "On-line failure detection and damping measurement of aerospace structures by random decrement signatures," Technical report NASA CR-2205, 75 pp.

Corneiro, M. C. (**2006**). "Can buildings be made earthquake-safe?," Science **312**, 204–206.

Crandall, S. (**1970**). "The role of damping in vibration theory," J. Sound Vib. **11**, 3–18.

Farrar, C. R., Doebling, S. W., and Nix, D. A. (**2001**). "Vibration-based structural damage identification," Philos. Trans. R. Soc. **359**, 131–149.

Field, E. H., Johnson, P. A., Beresnev, I. A., and Zeng, Y. (**1997**). "Nonlinear ground-motion amplification by sediments during the 1994 Northridge earthquake," Nature **390**, 599–601.

Guyer, R. A., and Johnson, P. A. (**1999**). "Nonlinear Mesoscopic elasticity: Evidence for a new class of materials," Phys. Today **52**(4), 30–35.

Guyer, R. A., and Johnson, P. A. (**2009**). *Nonlinear Mesoscopic Elasticity: The Complex Behaviour of Rocks, Soil, Concrete* (Wiley, New York).
HAZUS Technical Manual (**1999**). Federal Emergency Management Agency, Washington, DC, USA.
Herak, M., and Herak, D. (**2010**). "Continuous monitoring of dynamic parameters of the DGFSM building (Zagreb, Croatia)," Bull. Earthquake Eng. **8**(3), 657–669.
Hillers, G., Graham, N., Campillo, M., Kedar, S., Landès, M., and Shapiro, N. (**2012**). "Global oceanic microseism sources as seen by seismic arrays and predicted by wave action models," Geochem., Geophys., Geosyst. **13**(1), 1–19, doi:10.1029/2011GC003875.
Johnson, P. A., Bodin, P., Gomberg, J., Pearce, F., Lawrence, Z., and Menq, F. (**2009**). "Inducing *in situ*, nonlinear soil response applying an active source," J. Geophys. Res. **114**, B05304, doi:10.1029/2008JB005832.
Johnson, P. A., and Sutin, A. (**2005**). "Slow dynamics and anomalous nonlinear fast dynamics in diverse solids," J. Acoust. Soc. Am. **117**, 124–130.
Karabulut, H., and Bouchon, M. (**2007**). "Spatial variability and nonlinearity of strong ground motion near a fault," Geophys. J. Int. **170**, 262–274.
Kashima, T., and Kitagawa, Y. (**2006**). "Dynamic characteristics of an 8-story building estimated from strong motion records," in *Proc. First European Conference on Earthquake Engineering and Seismology*, Geneva, Switzerland, 3–8 September.
Kohler, M., Davis, P. A., and Safak, E. (**2005**). "Earthquake and ambient vibration monitoring of the steel-frame UCLA Factor building," Earthquake Spectra **21**, 715–736.
Lacouture, J.-C., Johnson, P. A., and Cohen-Tenoudji, F. (**2003**). "Study of critical behavior in concrete during curing by application of dynamic linear and nonlinear means," J. Acoust. Soc. Am. **113**(3), 1325–1332.
Luco, J. E., Trifunac, M. D., and Wong, H. L. (**1987**). "On the apparent change in dynamic behavior of a nine-story reinforced concrete building," Bull. Seismol. Soc. Am. **77**, 1961–1983.
Michel, C., and Guéguen, P. (**2010**). "Time–frequency analysis of small frequency variations in civil engineering structures under weak and strong motions using a reassignment method," Struct. Health Monit. **9**(2), 159–171.
Mikael, A., Guéguen, P., Bard, P.-Y., Roux, P., and Langlais, M. (**2013**). "The analysis of long-term frequency and damping wandering in buildings using the random decrement technique," Bull. Seismol. Soc. Am. **103**, 236–246.
Nasser, F., Li, Z., Martin, N., and Guéguen, P. (**2016**). "An automatic approach towards modal parameter estimation for high-rise buildings of multicomponent signals under ambient excitations via filter-free random decrement technique," Mech. Syst. Signal Process. **70–71**, 821–831.
Nayeri, R. D., Masri, S. F., Ghanem, R. G., and Nigbor, R. L. (**2008**). "A novel approach for the structural identification and monitoring of a full-scale 17-story building based on ambient vibration measurements," Smart Mater. Struct. **17**, 1–19.
Ohmachi, T., and Tahara, T. (**2011**). "Nonlinear earthquake response characteristics of a central clay core rockfill dam," Soils Found. **51**(2), 227–238.
Ostrovsky, L. A., and Johnson, P. A. (**2001**). "Dynamic nonlinear elasticity in geomaterials," Riv. Nuovo Cimento **24**(7), 1–46.
Pasqualini, D., Heitmann, K., TenCate, J. A., Habib, S., Higdon, D., and Johnson, P. A. (**2007**). "Nonequilibrium and nonlinear dynamics in Berea and Fontainebleau sandstones: Low-strain regime," J. Geophys. Res. **112**, B01204, doi:10.1029/2006JB004264.
Peng, Z., and Ben-Zion, Y. (**2006**). "Temporal changes of shallow seismic velocity around the Karadere-Düzce branch of the North Anatolian Fault and strong ground motion," Pure Appl. Geophys. **163**, 567–600.
Renaud, G., Le Bas, P.-Y., and Johnson, P. A. (**2012**). "Revealing highly complex elastic nonlinear (anelastic) behavior of Earth materials applying a new probe: Dynamic acoustoelastic testing," J. Geophys. Res.: Solid Earth **117**(B6), 2156–2202, doi:10.1029/2011JB009127.
Renaud, G., Riviére, J., Larmat, C., Rutledge, J. T., Lee, R. C., Guyer, R. A., Stokoe, K., and Johnson, P. A. (**2014**). "*In situ* characterization of shallow elastic nonlinear parameters with dynamic acoustoelastic testing," J. Geophys. Res. Solid Earth **119**(9), 6907–6923, doi:10.1002/2013JB010625.
Roux, P. (**2009**). "Passive seismic imaging with directive ambient noise: Application to surface waves on the San Andreas Fault (SAF) in Parkfield," Geophys. J. Int. **179**(1), 367–373.
Roux, P., Guéguen, P., Baillet, L., and Hamze, A. (**2014**). "Structural-change localization and monitoring through a perturbation-based inverse problem," J. Acoust. Soc. Am. **136**(5), 2586–2597.
Rutter, E. H. (**1983**). "Pressure solution in nature, theory and experiment," J. Geol. Soc. **140**, 725–740.
Sawazaki, K., Sato, H., Nakahara, H., and Nishimura, T. (**2009**). "Time-lapse changes of seismic velocity in the shallow ground caused by strong ground motion shock of the 200 Western-Tottori earthquake, Japan, as revealed from Coda deconvolution analysis," Bull. Seismol. Soc. Am. **99**(1), 352–366.
Skolnik, D., Lei, Y., Yu, E., and Wallace, J. W. (**2006**). "Identification, model updating, and response prediction of an instrumented 15-story steel-frame building," Earthquake Spectra **22**, 781–802.
Snieder, R., and Şafak, E. (**2006**). "Extracting the building response using seismic interferometry: Theory and application to the Milikan library in Pasadena, California," Bull. Seismol. Soc. Am. **96**(2), 586–598.
Stehly, L., Shapiro, N., and Campillo, M. (**2006**). "A study of the seismic noise from its long-range correlation properties," J. Geophys. Res. **111**, B10306, doi:10.1029/2005JB004237.
TenCate, J. A. (**2011**). "Slow dynamics of Earth materials: An experimental overview," Pure Appl. Geophys. **168**, 2211–2219.
Todorovska, M. I., and Al Rjoub, Y. (**2006**). "Effects of rainfall on soil-structure system frequency: Example based on poroelasticity and a comparison with full-scale measurements," Soil Dyn. Earthquake Eng. **26**, 708–717.
van der Elst, N. J., Brodsky, E. E., Le Bas, P. Y., and Johnson, P. A. (**2012**). "Auto-acoustic compaction in steady shear flows: Experimental evidence for suppression of shear dilatancy by internal acoustic vibration," J. Geophys. Res.: Solid Earth **117**(B9), 1–18, doi:10.1029/2011JB008897.
Wu, C., Peng, Z., and Assimaki, D. (**2009a**). "Temporal changes in site response associated with the strong ground motion of the 2004 Mw 6.6 Mid-Niigata earthquake sequences in Japan," Bull. Seismol. Soc. Am. **99**(6), 3487–3495.
Wu, C., Peng, Z., and Ben-Zion, Y. (**2009b**). "Non-linearity and temporal changes of fault zone site response associated with strong ground motion," Geophys. J. Int. **176**, 265–278.